Excited state charge separation in symmetrical alkenes

Zijlstra, Robert Wiebo Johan

Polarization of the Excited States of Twisted Ethylene in a Non-Symmetrical Environment

3.1 Introduction

For various reasons, the dynamic behavior of the photo-induced excited states of ethylenic systems has been the subject of numerous theoretical and experimental studies. For instance, interest in understanding cis-trans isomerization processes of ethylenic compounds in which the cis-trans isomerization of retinal, the key molecule in the mechanism of vision, is probably the most exciting example[1] and has contributed to the large number of studies performed on this class of compounds.

One of the most intriguing aspects of the behavior of the excited states of (symmetrical) alkenes is the existence of a polarized (charge separated) state, in which two electrons—unpaired and distributed in the initial biradical excited state—are localized at one side of the molecule, thus leading to the formation of a considerable dipole moment.

Both direct and indirect experimental evidence of the existence of such a suddenly polarized[2] 'phantom' state has been obtained from time resolved photo induced excitation experiments on tetraphenylethylene (TPE)[3-9] and several other alkenes[10-12], in which a polarized state could be detected in various solvents.

A remarkable observation in the experiments concerning TPE is the dependence of the lifetime of the polarized state on solvent polarity[5, 6], in which a decreasing lifetime with increasing solvent polarity was observed. In these studies, increased coupling due to an decreased energy gap between the twisted (D_{2d}) ground state and the more stabilized polarized excited state was suggested as a possible explanation for this observation. The occurrence of the polarization of TPE, in twisted geometries only, was deduced from the observation of a strong reduction of the quantum yield for formation of polarized excited TPE with increasing solvent viscosity[8] and by Resonance Raman spectroscopy[13]. The twisting around the central bond will be increasingly hindered and fluorescence from the—nearly planar—relaxed vertically excited state, will become the dominant relaxation pathway.

On the origin of the localized states it should be noted that after the vertical excitation of an electron from the D_{2h} ground state of ethylene, and other symmetrical alkenes, the C-C bond length will increase and a twist around the central C-C bond will be initiated[14]. On progressive twisting, three low lying singlet states arise, which at the perpendicular D_{2d} geometry ($\theta=90^0$) are denoted as N ($^1B_1$; ab), V($^1B_2$; a^2-b^2) and Z ($^1A_1$; a^2+b^2) and are sensitive to rotation around the C-C bond. The N state is destabilized going from the D_{2h} to the D_{2d} geometry, while the V and Z states are stabilized, coming close together at near perpendicular geometries and—in the Born-Oppenheimer approximation—cross for $\theta\approx80^0$. At and around the crossing V and Z are (nearly) degenerate and therefore wave functions of type V ± Z are equally acceptable, resulting in localized a^2 or b^2 states which will have considerable dipole moments. A theoretical description of the vacuum situation should be based on the appropriate (open shell, many determinant) wave functions and symmetry, i.e.V ± Z should have equal weights as long as the D_{2d} symmetry remains, and no dipole should exist.

Previous theoretical studies provided valuable insight into the possible polarization of the (near) perpendicularly twisted (D_{2d}) excited states of ethylene. CISD studies by Brooks and Schaefer III[15] showed that lowering the nuclear symmetry to C_s by pyramidalization of one of the two carbon centers leads to the build up of large dipole

moments due to considerable mixing between the —originally (D_{2d}) V and Z —states. MRCI studies of Buenker et al.[16, 17] have shown that combined pyramidalization and twisting of the central double bond leads to the formation of highly polarized states in the vicinity of the crossing of the Z and V state energy surfaces.

Since experimental results always are related to the condensed phase, it can be worthwhile to investigate whether solvent polarization on its own could be responsible for the lowering of the symmetry required for localization of these states. If the system is embedded in some polarizable medium, the transient a^2 or b^2 states can generate reaction potentials which may live sufficiently long to lift the degeneracy and stabilize one with respect to the other, without lowering the symmetry of the nuclear arrangement.

To that end the Direct Reaction Field approach[18-20] has been applied, which allows various ways of modeling solvent effects, e.g. representing the "solvent" by (sets of) discrete semi-classical solvent molecules (distributed multipoles + polarizabilities) or by a dielectric continuum, or both. The model can treat ab initio RHF, ROHF, GVB, MCSCF and CI wave functions for ground and excited states in equilibrium and non-equilibrium situations, while the solute/solvent interactions may be accounted for fully self consistent or as first-order perturbations. For solvent effects from the discrete model at finite temperatures Monte Carlo sampling of the solvent's degrees of freedom is provided. All this was implemented in the ab initio package HONDO 8.1[21]. A general description of the DRF model will be given in the next paragraph.

In this chapter it was decided to use the dielectric model only[22], although it has been pointed out that this is not without problems[23]. Moreover, since ab initio calculations on TPE are not feasible on the level of theory required, ethylene has been used as model compound.

3.2 The DRF Model

3.2.1 Introduction

Solvent effects play a very important role in chemistry since most chemical reactions and biological processes take place in solutions. The properties of molecules and the interactions between them in solution can differ greatly from the properties and interactions in vacuum, the state to which most quantum chemical calculations refer. Including solvent effects in quantum chemical calculations by adding quantum mechanically treated solvent molecules would lead to an enormous increase in computational cost. A more fruitful approach is the development of a mixed quantum mechanical/classical model in which the system of interest (the solute) is treated quantum mechanically and the surrounding solvent is treated classically.

The first attempts to combine a quantum mechanical system with classical surroundings were based on a dielectric continuum description[24] of the solvent. In these models the (quantum mechanical) solute is placed in a cavity in a dielectric continuum. These models have been used with reasonable success, however there are important limitations. They employ a macroscopic property of the solvent, the dielectric constant, to model the interactions on a microscopic scale, which means that they can never accurately

describe specific solvent-solute interactions e.g. hydrogen bonding[25, 26]. Another drawback is the need to reparameterize the model for each different solvent.

These difficulties can be resolved by using explicit solvent models. A number of these have been developed over the last years[27, 28]. Most of them are based on a Lennard-Jones type force field for the dispersion and short range repulsion terms, and point charges for modeling electrostatic effects. Recently, polarization effects were added to these models to include induction interactions[28-30], however the explicit polarizabilities are not used for modeling the dispersion. The Lennard-Jones parameters are fitted to ground state interaction energies and so no distinction can be made between dispersion interaction in the ground state and the excited states without reparameterizing for the excited states.

These problems are all omitted in the Direct Reaction Field (DRF)[18-20] model. The model is summarized in Figure 3.1. The quantum system is surrounded by discrete classical systems (A, B,.....) modeling the first few solvent shells. These solvent shells can optionally be surrounded by a dielectric continuum for modeling bulk effects. The total energy of the system consisting of a quantum mechanically described solute and a discrete classical solvent is given by :

$$\Delta U^{discr} = \Delta U^{QM} + \Delta U^{MM} + \Delta U^{QM/MM} \qquad \textbf{(3.1)}$$

in which ΔU^{QM} is the expectation value of the vacuum Hamiltonian over the nonvacuum wave function, ΔU^{MM} represents the interactions between the classical subsystems and $\Delta U^{QM/MM}$ is the interaction between the quantum system and the classical surroundings.

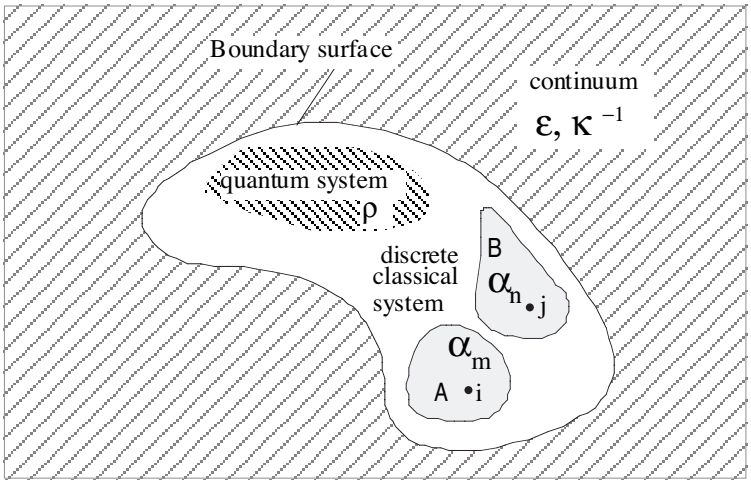

Figure 3.1 DRF model for the condensed phase.

3.2.2 Classical Interactions in the DRF Model

The interactions between classical solvent molecules are modeled by point charges, radii and polarizabilities. These parameters can all be derived from the monomer properties, either from experiments or from calculations. Point charges can be derived from ab initio wave functions on the monomers (A,B,....) using a dipole preserving population analysis[31] or by fitting charges to the electrostatic potential[32]. For the radii experimental values like Van der Waals radii can be used, but calculated values can also be obtained (e.g. from the quadrupole moment or from polarizabilities). Atomic

polarizabilities can be obtained by fitting them to experimental or calculated molecular polarizabilities in a procedure developed by Thole[33, 34].

The classical interactions in the DRF model can be written as :

$$\Delta U^{MM} = \sum_{\substack{i\in A, j\in B \\ A>B}} q_i^A \, \upsilon_{ij} \, q_j^B + \frac{1}{2} \sum_{\substack{i\in A, j\in B \\ A,B \\ rs\notin AB}} q_i^A \, f_{ir} \, A_{rs} \, f_{sj} \, q_j^B + \Delta U_{disp}^{MM} + \Delta U_{rep}^{MM} \qquad \textbf{(3.2)}$$

with $\upsilon_{ij} = \frac{1}{|r_i - r_j|}$, the Coulomb potential in **j**, brought about by a source in **i** and $f_{ij} = -\nabla_j V_{ij}$ is the corresponding electric field. The first two terms are the Coulomb interaction and the induction interaction (also called 'screening of the electrostatic interaction'). q_i^A is the i-th point charge of classical group A. The A_{rs} are elements of the matrix $\mathbb{A}$, which can be considered as the total polarizability of a system of molecules (see below). It should be noted that in Equation 3.2 all interactions within monomers are set to zero.

For the classical dispersion interaction, the Slater-Kirkwood expression[35] is used:

$$\Delta U_{disp}^{MM} = \sum_{i<j} \frac{1}{4R^6} \frac{Tr\left(\alpha_i \, \mathbb{t}(\mathbf{i};\mathbf{j})^2 \, \alpha_j\right)}{\left(\sqrt{\alpha_i/n_i} + \sqrt{\alpha_j/n_j}\right)} \qquad \textbf{(3.3)}$$

in which $\mathbb{t}(\mathbf{i};\mathbf{j})$ is the interaction tensor for the induced dipoles at **i** and **j**. For the short range repulsion the CHARMM[36] expression is used :

$$\Delta U_{rep}^{MM} = \sum_{i<j} \frac{3}{4} \frac{\bar{\alpha}_i \, \bar{\alpha}_j \, (r_i + r_j)^6}{\left(\sqrt{\bar{\alpha}_i/n_i} + \sqrt{\bar{\alpha}_j/n_j}\right)} r_{ij}^{-12} \qquad \textbf{(3.4)}$$

in which $\bar{\alpha}_i$, n_i, and r_i are the isotropic polarizability, number of valence electrons, and radius of atomic center i, respectively, and r_{ij} is the distance between centers i and j. The integral number of valence electrons of an atom and the same atomic polarizabilities that go into the electrostatic, response, and dispersion terms are used, leaving only the atomic radii as independent parameters.

3.2.3 Coupling of the Classical and Quantum Mechanical Systems

The static electric field, brought about by the point charges of the classical groups, can easily be introduced in the solute Hamiltonian. Adding reaction field effects due to interaction with classical polarizabilities however, is more difficult. The coupling of the quantum mechanical solute and the polarizable solvent system can be done by performing a so called coupled-SCF procedure described by Thompson[29] in which the wave function has to be solved from a nonlinear equation:

$$\left[\hat{H}^{Q} + \hat{H}^{RF}\left(\Phi_Q\right)\right]\Phi_Q = E\left(\Phi_Q\right)\Phi_Q \qquad \textbf{(3.5)}$$

$\hat{H}^{Q}$ is the normal vacuum Hamiltonian, $\hat{H}^{RF}$ is the reaction field Hamiltonian which is dependent on the wave function itself because it includes the dipole moments induced by the quantum system (in the classical polarizable system). This nonlinear equation has to be solved in an iterative scheme in which first the induced moments are calculated:

$$\mu_p = \alpha_p \left[f_p + \sum_{p \neq q} f(m_q,p) + f_p^Q (\Phi_Q) \right] \qquad \textbf{(3.6)}$$

f_p is the static field felt in p, $f(m_q, p)$ is the field in p due to a (classically induced) moment in q and f_p^Q is the field in p due to the quantum system. These induced moments are put into the reaction field hamiltonian $\hat{H}^{RF}$, which is then used to calculate a new wave function which is in turn used to generate new induced moments, etc., until convergence is reached. In this way the solute feels the average response of the classical polarizabilities to the field due to the solute (i.e., the Average Reaction Field) and the induction interaction between the quantum system and the classical system can be calculated.

A more elegant approach is presented by the *direct* reaction field model (DRF)[18-20, 31] in which the effect of the solvent polarizability is introduced directly into the vacuum solute hamiltonian (H^0) :

$$H = H^0 + H^{es} + H^{rf} \qquad \textbf{(3.7)}$$

with H^{es} and H^{rf} the electrostatic and reaction potential *operators*. The interaction energy between a quantum mechanically described solute and a system of (classical) point charges and polarizabilities $\mathbb{A}$ (i.e. the solvent, see below)—for a single determinant, closed shell wave function —is given by :

$$\begin{aligned}
\Delta U_{int}^{QM/MM} = & \sum_{A,i,j} q_i^A \vartheta_{ij} Z_j + e \sum_{A,i} q_i^A \langle \vartheta \rangle_i + \\
& \sum_{A,i,j,r,s} q_i^A f_{ir} A_{rs} f_{sj} Z_j + e \sum_{A,k,j,r,s} q_j^A f_{jr} A_{rs} \langle f(s;k) \rangle + \\
& \frac{1}{2} \sum_{i,j,r,s} Z_i f_{ir} A_{rs} f_{sj} Z_j + e \sum_{i,k,r,s} Z_i f_{ir} A_{rs} \langle f(s;k) \rangle + \\
& \frac{\gamma}{2} e^2 \sum_{k,r,s} \langle f(k;r) A_{rs} f(s;k) \rangle + \frac{1}{2} e^2 \sum_{k,l,r,s} \langle f(k;r) \rangle A_{rs} \left(1 - \frac{\gamma}{2} P_{12} \right) \langle f(s;l) \rangle \\
& + \Delta U_{rep}^{QM/MM}
\end{aligned} \qquad \textbf{(3.8)}$$

In the first two terms of equation 3.8 we see the electrostatic interactions of nuclei and electrons with the point charges. The third term contains the interactions of the point charges with the dipoles induced by the nuclei and vice versa. The fourth represents the

interaction between the point charges and the dipoles induced by the electrons and vice versa. The fifth and sixth terms are the screening of the nuclear repulsion and attraction respectively (part of the induction). The seventh term contains the interaction of each electron with its own induced dipoles, the eighth is the interaction of each electron with the dipoles induced by the other electrons, hence it is a two electron term. This term contains the induction interaction and part of the dispersion. The scaling factor, γ, is for the dispersion which is discussed below, and P_{12} is the permutation operator. If one takes $\gamma = 0$ term seven disappears and in term eight only the induction part remains. In order to distinguish between source and recipient in the expectation values of the field—e.g. $\langle f(k;s) \rangle$, i.e. the electric field at **s** due to electron k—the electron labels (k,l) and the electronic charge (e) have been made explicit so as to avoid ambiguity in the signs of the various terms. In equation 3.8 the cost of inducing all the dipoles in the classical system has already been included.

The repulsion term in equation 3.8 is the same as in equation 3.4, although the radii of the QM atoms may optionally be obtained "on the fly" (i.e. when needed) instead of fixing them on their vacuum values.

The difference of the expectation values

$$\langle \Psi | H | \Psi \rangle - \langle \Psi^0 | H^0 | \Psi^0 \rangle + \Delta U_{rep}^{QM/MM} = \Delta U_{int}^{QM/MM} \qquad \textbf{(3.9)}$$

contains all first and second order contributions usually obtained when Ψ refers to a super molecule SCF calculation, and more. The expectation value of H^{rf} can be rewritten as:

$$\begin{aligned} \langle H^{rf} \rangle &= -\frac{1}{2} \langle f^{\dagger} \mathbb{A} f \rangle = -\frac{1}{2} \langle f \rangle^{\dagger} \mathbb{A} \langle f \rangle - \frac{1}{2} \left\{ \langle f^{\dagger} \mathbb{A} f \rangle - \langle f \rangle^{\dagger} \mathbb{A} \langle f \rangle \right\} \\ &= \Delta U_{DRF}^{ind} + \Delta U_{DRF}^{disp} \end{aligned} \qquad \textbf{(3.10)}$$

The first term in equation 3.10 is the DRF induction interaction. The term between { }, the difference between the expectation value of the DRF hamiltonian and the average reaction field term, is the *unscaled* DRF dispersion interaction. It has been shown to be just the difference between the screened self energy and the screened exchange contribution (see equation 3.8). Moreover it has been shown that this expression approximately equals the second order perturbation theory (SOP) expression for dispersion, apart from a scaling factor[26, 37]

$$\Delta U_{disp}^{SOP} \approx \left(\frac{E_{solvent}^{i}}{E_{solute}^{i} + E_{solvent}^{i}} \right) \Delta U_{disp}^{DRF} = \gamma \, \Delta U_{disp}^{DRF} \qquad \textbf{(3.11)}$$

where E_{solute}^{i} and $E_{solvent}^{i}$ are the ionization energies of the quantum mechanical solute and the classical solvent respectively.

The reaction field operator was redefined accordingly[26, 37] i.e. by scaling with γ the integrals for screening of the one-electron self energy and of the two-electron

exchange contributions (see also equation 1.8). This is only possible if the exchange interaction is explicitly under control, i.e. only for single determinant wave functions. When using $\gamma = 0$ the wave function does not feel the effect of dispersion with the classical system and the method renders in fact the Average Reaction Field (ARF) method rather than the DRF approach. This will thus lead to the same induction as is obtained when using the coupled-SCF method described above. With $\gamma \neq 0$ the quantum system does feel the effect of dispersion which will modify the wave function, this in turn will lead to a somewhat different induction interaction.

The matrix $\mathbb{A}$—used in equation 3.2, 3.8 and 3.10—is a (super)matrix representing the total linear response of the complete discrete classical part, in which all parts interact self consistently. Taking a set of points $\{\mathbf{p}\}$ with polarizabilities $\{\alpha_p\}$ in a uniform electric field $\mathbf{F}^0$ we have for the induced dipole moment in point $\mathbf{p}$:

$$\mathbf{m}_p = \alpha_p \left(\mathbf{F}^0(\mathbf{p}) - \sum_{q \neq p}^{N^{pol}} t(\mathbf{p};\mathbf{q})\, \mathbf{m}_q \right) \qquad \textbf{(3.12)}$$

A formal solution for $\{\mathbf{m}_p\}$ can be found by collecting the N^{pol} equations into a single super matrix equation of dimension N^{pol} x N^{pol}:

$$\mathbf{M} = \alpha \left(\mathbf{F}^0 - \mathbb{T}\, \mathbf{M} \right) \qquad \textbf{(3.13)}$$

where $\mathbf{F}^0$ and $\mathbf{M}$ are $3N^{pol}$-dimensional vectors, and α and $\mathbb{T}$ are square $3N^{pol}$ x $3N^{pol}$ matrices. The super vectors and matrices are blocked into $3N^{pol}$ and $3N^{pol}$ x $3N^{pol}$ elements, respectively: $\mathbf{M}_p = \mathbf{m}_p$, $\alpha = \alpha_p \delta_{pq}$, $\mathbb{T}_{pq} = t(\mathbf{p};\mathbf{q})(1-\delta_{pq})$, and δ_{pq} is the Kronecker delta. Then

$$\mathbb{A} = \left(\alpha^{-1} + \mathbb{T} \right)^{-1} \qquad \textbf{(3.14)}$$

may be considered as an ordinary polarizability matrix (but of an N^{pol} membered system):

$$\mathbf{M} = \mathbf{F}\,\mathbb{A} = \mathbf{F} \left(\alpha^{-1} + \mathbb{T} \right)^{-1} \qquad \textbf{(3.15)}$$

$\mathbb{A}$ is obtained either by an exact matrix inversion or by solving the associated linear equations by iteration. It should be noted that equation (3.15) is a self consistent solution for any field, e.g. the electric field of QM during any stage of e.g. the Hartree-Fock procedure, and can expressed in terms of integrals over any basis set, which can be added to the vacuum Hamiltonian.

The $\{t(\mathbf{p};\mathbf{q})\}$ are, when appropriate, screened according to the method described by Thole[31] in which (atomic) polarizabilities are taken as related to (model) charge distributions, the widths of which are related to the $\{\alpha_p\}$. This leads also to a consistent screening of the potentials and fields of interaction for overlapping charge distributions.

In general the polarizabilities are constructed following Thole's original recipe and parametrization for obtaining (molecular) polarizabilities with experimental accuracy. This model has been reparametrized, also for computed polarizabilities from specific basis sets[34]. The advantage of this way of treating the relay matrix is that only atomic polarizabilities are needed as input, while changes in geometry will be automatically reflected in $\mathbb{A}$. Optionally one may reduce parts of $\mathbb{A}$ first to group polarizabilities so as to reduce the dimensionality of the problem. For a detailed description of the DRF model and its implementation the reader is referred to the paper published recently by de Vries *et al.*[20], this paper also descibes the extension of the DRF model with a third level of detail, a dielectric continuum surrounding the first few discrete solvent layers.

Thus in the DRF model the energy can be obtained as the expectation value of the DRF hamiltonian without the need for an iterative solution scheme. Furthermore the electrons in the quantum system are directly correlated with the classical charge distributions modeled by polarizabilities, thus the dispersion interaction between classical and quantum system is included. When a wave function for an excited state is used instead of that for the ground state, the dispersion interaction will be different, so the DRF model allows to model the effect of dispersion on spectral transitions.

3.3 Computational Details

In this study, only the dielectric model has been used to simulate the effect of a non-symmetrical solvent shell around the ethylene molecule. The adopted geometry of ethylene is shown in figure 3.2.

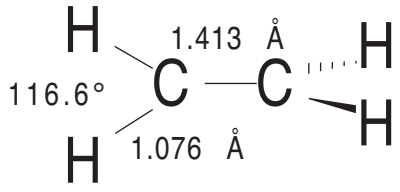

Figure 3.2 Adopted ethylene geometry.

Calculations in vacuum should yield symmetric wave functions with zero dipole moments for both ground and excited states at any point of the twisting energy surface. In the calculations presented here the Dunning-Huzinaga double valence (DZV) basis was used. The singlet ROHF vectors for the N state were used to define the reference configuration in an all valence CISD (~ 60.000 determinants involved). For all rotation angles, the CI wave functions yielded perfectly zero dipole moments for both the ground and the investigated excited states.

A non-symmetrical reaction potential was obtained from the dielectric continuum with various dielectric constants, generated by a localized charge density for the near 90° twist angles, which was obtained from a closed shell RHF procedure, in which an a^2 solution was obtained with a considerable dipole moment (μ_z ~ 4.0 Debye). Although physically incorrect in vacuo, this localized wave function yields a reasonable electron density distribution for a polarized excited state.

For the necessary boundary between discrete and continuum parts a Connolly surface[38] defined at twice the Van der Waals radii of the ethylene atoms around the geometry of the solute at hand, was taken. This distance was considered large enough to avoid unphysical polarizations[23]. The point density was chosen such that about 600 surface elements resulted. Reaction potentials are obtained by solving numerically appropriate Poisson equations. At the selected geometries, self consistent reaction potentials from the "closed shell" RHF (a^2) wave functions were obtained and added to the one-electron Hamiltonian in the CISD calculations.
This procedure was performed for ε=2.0, 4.0, 6.0 and 10.0, which are typical values for a range of non-hydrogen bonding organic solvents with increasing polar behavior.

3.4 Results and Discussion

The vacuum energies of the states of interest of ethylene were obtained from the first series of calculations. Since Buenker et. al. showed the crossing surface between the Z and V states of ethylene, at a twist angle of approximately 80° for the central bond[17], to be the twist region highly sensitive to polarization, the investigation was restricted to the 70-90° twist area.

In the CISD calculations, all 12 valence electrons were included from the reference singlet ROHF wave function and were allowed to excite into the complete virtual space (17 virtuals) thus leading to a CI space of 60.480 determinants. Results are given in table 3.1.

twist angle (°)	70	75	80	85	90
N	-78.12256	-78.11431	-78.10736	-78.10260	-78.10088
Z*	-77.96553	-77.96810	-77.96996	-77.97108	-77.97145
V*	-77.94613	-77.95858	-77.96858	-77.97519	-77.97753

Table 3.1 CISD vacuum energies (a.u.) of the N, Z and V state of ethylene in the 70-90° twist range (* See figure 3.4 for graphical representation of the potential energy surface of the Z and V states)

ε	Ψ_{RHF} (a.u.)	μ_z (Debije)	Ψ_{ROHF} (a.u.)	μ_z (Debije)
vacuo	-77.80991	+ 3.760	-77.93843	0.000
2.0	-77.81122	+ 3.887	-77.93715	+0.095
4.0	-77.81212	+ 3.972	-77.93625	+0.161
6.0	-77.81247	+ 4.006	-77.93590	+0.186
10.0	-77.81278	+ 4.034	-77.93563	+0.208

Table 3.2 SCF energies (a.u.) and dipole moments (Debije) of the Ψ_{RHF} and Ψ_{ROHF} singlet wave functions at different values of ε

These CI expansions lead to perfectly zero dipole moments for all states at all investigated geometries, which shows that these CI expansions can reproduce the desired symmetrical wave functions in vacuo. At this point, these findings differ from those by

Schaefer III and Brooks[15], who found non zero dipole moments for the D_{2d} Z and V states in similar expansions. Results of the reaction field calculations with the closed and open shell RHF wave functions in the (non-)equilibrium reaction potentials of the former are shown in table 3.2.

It should be noted that only geometries near 90˚ are able to yield such a polarized RHF wave function, since increasing overlap between the "p_z" orbitals on the carbon centers on decreasing twist angles will lead to a delocalized RHF solution.

	"μ^+"				"μ^-"			
twist angle	E_{tot} (a.u.)	μ_z (D)	"a^2"	"b^2"	E_{tot} (a.u.)	μ_z (D)	"a^2"	"b^2"
70˚								
ε=2.0	-77.96463	+0.657	.669	-.566	-77.94481	-0.349	.507	.618
ε=4.0	-77.96435	+1.073	.700	-.526	-77.94377	-0.592	.467	.649
ε=6.0	-77.96431	+1.226	.710	-.512	-77.94355	-0.669	.452	.660
ε=10.0	-77.96431	+1.353	.718	-.499	-77.94297	-0.731	.439	.669
75˚								
ε=2.0	-77.96751	+1.183	.720	-.502	-77.95716	-0.894	.459	.687
ε=4.0	-77.96744	+1.802	.764	-.428	-77.95601	-1.317	.383	.734
ε=6.0	-77.96795	+1.997	.777	-.403	-77.95553	-1.437	.357	.747
ε=10.0	-77.96818	+2.148	.787	-.382	-77.95510	-1.522	.337	.757
80˚								
ε=2.0	-77.97099	+2.885	.856	-.165	-77.96672	-2.592	.137	.848
ε=4.0	-77.97211	+3.090	.865	-.108	-77.96513	-2.599	0	.855
ε=6.0	-77.97270	+3.143	.866	-.097	-77.96448	-2.575	0	.856
ε=10.0	-77.97314	+3.185	.867	-.088	-77.96392	-2.551	0	.857
85˚								
ε=2.0	-77.97534	+2.191	.805	.340	-77.96954	-1.896	.352	-.805
ε=4.0	-77.97638	+2.762	.843	.235	-77.96823	-2.266	.248	-.840
ε=6.0	-77.97686	+2.895	.851	.208	-77.96766	-2.322	.846	-.221
ε=10.0	-77.97731	+2.991	.857	.188	-77.96714	-2.349	.201	-.851
90˚								
ε=2.0	-77.97719	+1.781	.774	.417	-77.96811	-1.474	.772	-.423
ε=4.0	-77.97799	+2.465	.824	.313	-77.96858	-1.941	.319	-.817
ε=6.0	-77.97823	+2.647	.835	.285	-77.96802	-2.047	.291	-.828
ε=10.0	-77.97858	+2.778	.843	.263	-77.96751	-2.107	.269	-.835

Table 3.3 CISD total energies (a.u.), dipole moments (Debije) and CI coefficients of both examined (polarized) excited states of twisted ethylene

A remarkable observation is that the energy gap between the closed shell and the open shell wave functions at the HF level yields a reasonable estimate of the energy gap between the ground state and the 'polarized excited state' (0.128 a.u at the HF level in vacuo against 0.129 a.u. at the CISD level with singlet open shell orbitals as reference, see table I and II for actual values). Furthermore, when using the polarized closed shell orbitals in an all valence CISD expansion at the D_{2d} geometry in vacuo, an energy similar

to those of the symmetrical first excited state is obtained (E_{CI} = -77.97897 a.u., μ_z = 3.232 Debye for this polarized state).

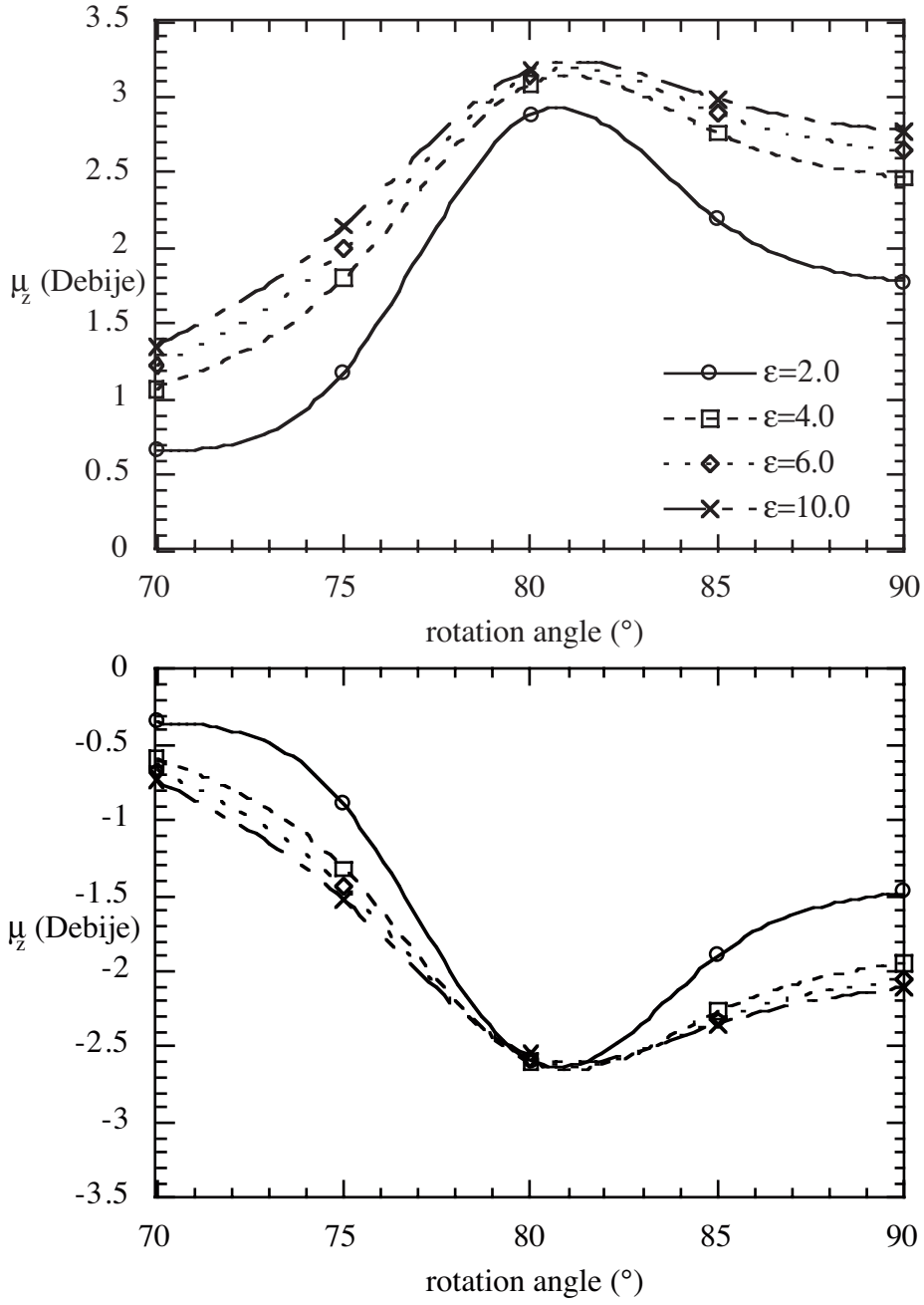

Figure 3.3 Polarized continuum induced dipole moments (Debije) of the two ethylenic excited states of interest on progressive twisting at various values of ε.

The total energies (E_{CI} + E_{DRF}) of the CISD expansion in the singlet ROHF orbitals of the three lowest lying states in the non-equilibrium reaction potentials, as well as the CI coefficients for the a^2 and b^2 contributions of the first two excited states are reported in table 3.3.

As can be seen from the CI coefficients, strong polarization occurs in the vicinity of the crossing of the 'pure' Z and V states in vacuo. This is emphasized in figure 3.3, which shows the dipole moments of the first two excited states in the 70-90° twist angle region.

A most remarkable feature from the observed dipole moments is the inability of the weak dielectric to maintain the large dipole moment on progressive twisting beyond the 80° point. From these findings, the conclusion can be made that for nonpolar solvents the weak electrostatic interactions with the solute are too small to sufficiently stabilize the polar state after formation. This can also be related to the total energies ($E_{CI}+E_{DRF}$) of the investigated excited states. In comparison with the vacuum CI energies of the non-localized Z and V states, all lowest lying polarized states except for ε=2.0 are stabilized relative to the vacuum lowest lying state (figure 3.4).

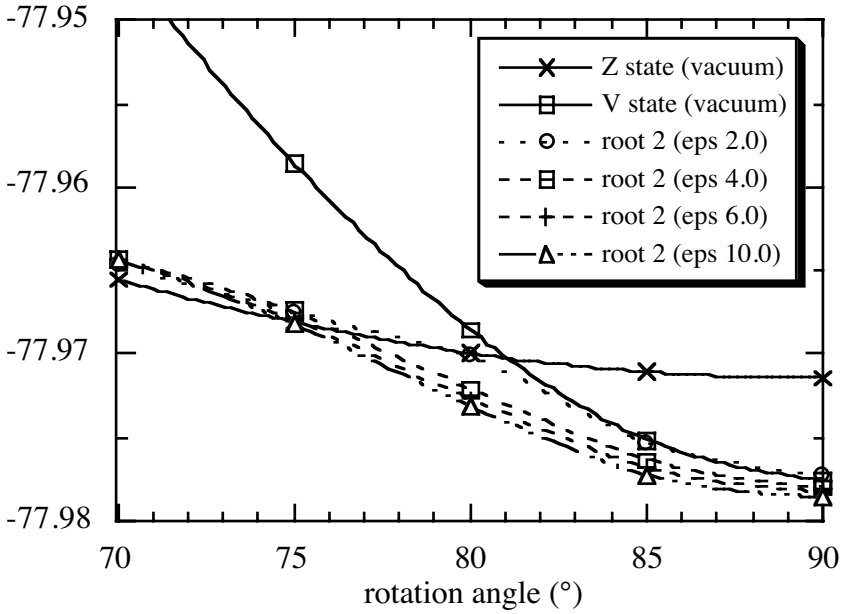

Figure 3.4 Total energies (a.u.) of embedded lowest excited states (dashed lines) and vacuum energies of the two excited states of interest (solid lines)

Another interesting observation when examining the CI coefficients of the excited states along the twisting coordinate is the switch of the dipole moment with positive sign from a "V state symmetry" ($c_1.a^2-c_2.b^2$) for twist angles α≤80° to a "Z state symmetry" ($c_1'.a^2+c_2'.b^2$), the state with the positive dipole moment always being the lowest in energy since they couple favorably with the external potential.

Figure 3.5 shows that this can be seen in terms of an avoided crossing between these states, in which the solvent asymmetry provides the required coupling for the occurrence of the avoided crossing of the Z and V state. This coupling of the dipole moment with the state lowest in energy has, to the best of our knowledge, not been reported in earlier studies.

Finally, investigation of the energy gap between the polarized excited states and the twisted ground state in the D_{2d} symmetry shows a significant lowering in energy of these

states in comparison with the vacuum energies, which is in agreement with earlier made assumptions.

It should be noted that the solvent model applied here is a simulation of an equilibrium situation, which especially for short-living polarized states (lifetime within the limit of the relaxation time of the solvent) in fact leads probably to an overestimation of the stabilizing effect from the solvent. On the other hand, the distance between the ethylene charge distribution and the boundary is so large, that the reaction field will be too small to account for the total electrostatic part of the solvation energy[23].

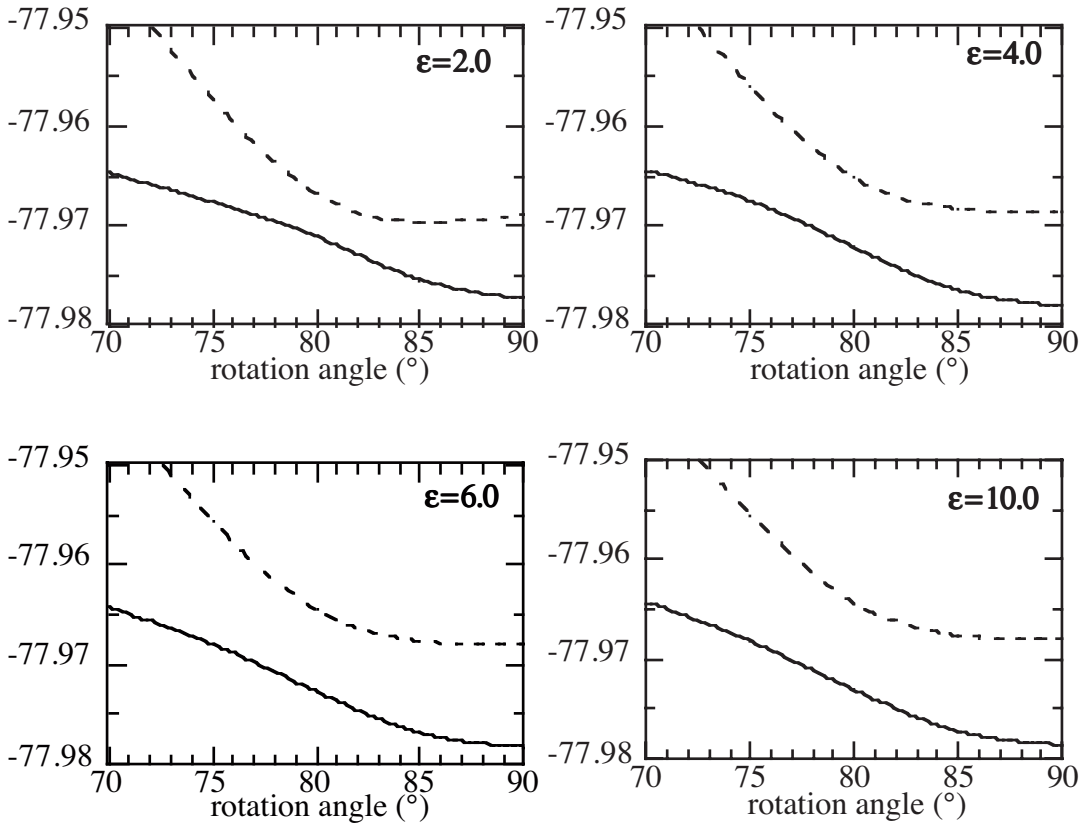

Figure 3.5 Total energies (a.u.) of second (solid line) and third root (dashed line) of ethylene as a function of rotation angle in various dielectrics.

DRF calculations in which discrete, classically described solvent layers with explicit molecular polarizabilities are used as a model for the first solvent shells have shown to give a quantitatively correct description of the various contributions in the solvent-solute interactions[26]. The results of this study are presented in the next chapter.

It can also be expected that symmetrical alkenes with stronger polarizable functional groups (like tetrachloro- or tetraphenylethylene) will show a more explicit behavior on the changes in solvent polarity. Unfortunately, the bulk of the theoretical investigations described in this thesis had to be limited to ethylene due to the unfeasability of the calculations on larger systems at similar levels of theory.

3.5 Conclusion

The presence of solvent layers with low symmetry around the twisted excited states of ethylene, here modeled by a dielectric in equilibrium with a prepared polarized state, effectively leads to large charge separations in the vicinity of the crossing intersection between these low lying excited (Z and V) states of ethylene. For dielectrics modeling (weakly) polar solvents, the energy of the lowest polarized excited state is stabilized relative to the pure Z and V states in vacuo. This is emphasized by the remaining dipole moments for those states on progressive twisting beyond the 80˚ point. The strong decrease in dipole moment on progressive twisting, together with the lack of stabilization of the polar state for a dielectric with ε=2.0 suggests that a relatively strongly polar compound in the various contributions of the solvation stabilization is needed to trap the polarized states in the near perpendicular geometries of the ethylene.

The lowest lying polarized state switches from V to Z symmetry around the 80˚ twisting point of the central bond (the crossing region of the Z and V *in vacuo* potentials), which is in nice agreement with earlier findings. The dipole moment of both states changes from sign when the avoided crossing has taken place.

The intriguing features of the abovementioned observations justify a more detailed description of the solvent, i.e. modelling the solvent by means of classically described discrete polarizable solvent molecules, to investigate whether these remarkable findings still hold in a more sophisticated treatment of the simulation. Especially the fact that a *polarized* dielectric had to be used to induce the symmetry breaking in the ethylene excited states may have biased the outcome and findings of this study, demands a more refined investigation. Therefore, the next chapter will be dedicated to the behaviour of the near-perpendicular excited states of ethylene in various solvents modelled by discretely described solvent shells in equilibrium with non-polarized ethylene.

3.6 References

1. Q. Wang, R.W. Schoenlein, L.A. Peteanu, R.A. Mathies and C.V. Shank, Science, **266**, 422-424 (1994).
2. V. Bonacic-Koutecky, P. Bruckmann, P. Hiberty, J. Koutecky, C. Leforestier and L. Salem, Angew. Chem., Int. Ed. Engl., **14**, 575-576 (1975).
3. W. Schuddeboom, S.A. Jonker, J.M. Warman, M.P. de Haas, M.J.W. Vermeulen, W.F. Jager, B. de Lange, B.L. Feringa and R.W. Fessenden, J. Am. Chem. Soc., **115**, 3286-3290 (1993).
4. B.I. Greene, Chem. Phys. Lett., **79**, 51-53 (1981).
5. C.L. Schilling and E.F. Hilinski, J. Am. Chem. Soc., **110**, 2296-2298 (1988).
6. J. Morais, J. Ma and M.B. Zimmt, J. Phys. Chem., **95**, 3885-3889 (1991).
7. Y-P. Sun and C.E. Bunker, J. Am. Chem. Soc., **116**, 2430-2433 (1994).
8. J. Ma and M.B. Zimmt, J. Am. Chem. Soc., **114**, 9723-9724 (1992).
9. E. Lenderink, K. Duppen and D.A. Wiersma, J. Phys. Chem., **99**, 8972-8977 (1995).
10. J. Saltiel, J. Am. Chem. Soc., **89**, 1036-1037 (1967).
11. J. Saltiel, D-H. Ko and S.A. Fleming, J. Am. Chem. Soc., **116**, 4099-4100 (1994).
12. D.B. Toublanc, R.W. Fessenden and A. Hitachi, J. Phys. Chem., **93**, 2893-2896 (1989).
13. T. Tahara and H. Hamaguchi, Chem. Phys. Lett., **217**, 369-374 (1994).
14. R.S. Mulliken, Phys. Rev., **41**, 751-758 (1932).
15. B.R. Brooks and H.F Schaefer III, J. Am. Chem. Soc., **101**, 307-311 (1979).
16. R.J. Buenker and S.D. Peyerimhoff, Chem. Phys., **9**, 75-89 (1976).
17. R.J. Buenker, V. Bonacic-Koutecky and L. Pogliani, J. Chem. Phys., **73**, 1836-1849 (1980).
18. P. Th. van Duijnen, A.H. Juffer and H.P. Dijkman, J. Mol. Struct. (THEOCHEM), **260**, 195-205 (1992).
19. B.T. Thole and P. Th. van Duijnen, Theor. Chim. Acta, **55**, 307-318 (1980).
20. A.H. de Vries, P.Th. van Duijnen, J.A.C. Ruhlmann, J.P. Dijkman, H. Merenga and B.T. Thole, J. Comp. Chem., **16**, 37-55 (1995).
21. M. Dupuis, A. Farazdel, S.P. Karma and S.A. Maluendes, *HONDO: A General Atomic and Molecular Electronic Structure System*, in: MOTECC, Ed: E. Clementi, ESCOM, Leiden, The Netherlands, 1990.
22. A.H. Juffer, E.F.F. Botta, B.A.M. van der Keulen, A. van der Ploeg and H.J.C. Berendsen, J. Comput. Phys., **97**, 144-171 (1991).
23. A.H. de Vries, P. Th. van Duijnen and A.H. Juffer, Int. J. Quant. Chem., Quant. Chem. Symp., **27**, 451-466 (1993).
24. J. Tomasi and M. Persico, Chem. Rev., **94**, 2027-2094 (1994).
25. M. Karelson and M.C. Zerner, J. Am. Chem. Soc., **112**, 9405-9406 (1990).
26. A.H. de Vries and P. Th. van Duijnen, Int. J. Quant. Chem., **57**, 1067-1076 (1996).
27. J. Gao and X. Xia, Science, **258**, 631-635 (1992).
28. J. Gao, Theor. Chim. Acta, **96**, 151-156 (1997).
29. M.A. Thompson and G.K. Schenter, J. Phys. Chem., **99**, 6374-6386 (1995).

30. M.A. Thompson, J. Phys. Chem., **100**, 14492-14507 (1996).
31. B.T. Thole and P. Th. van Duijnen, Theor. Chim. Acta, **63**, 209-221 (1983).
32. C.M. Breneman and K.B. Wiberg, J. Comp. Chem., **11**, 361-373 (1990).
33. B.T. Thole, Chem. Phys., **59**, 341-350 (1981).
34. P. Th. van Duijnen and M. Swart, J. Phys. Chem. A, **102**, 2399-2407 (1998).
35. J.C. Slater and J.G. Kirkwood, Phys. Rev., **37**, 682-697 (1931).
36. B.R. Brooks, R.E. Bruccoleri, B.D. Olafsson, D.J. States, S.J. Swaminathan and M. Karplus, J. Comp. Chem., **4**, 187-217 (1983).
37. P. Th. van Duijnen and A.H. de Vries, Int. J. Quant. Chem., **60**, 1111-1132 (1996).
38. M.L. Connolly, Science, **221**, 709-713 (1983).